

Evaluation of microwave processed glass–ceramic coating on nimonic superalloy substrate

S. Das ^{*}, A.K. Mukhopadhyay, S. Datta, D. Basu

Central Glass and Ceramic Research Institute, 196, Raja S.C. Mullick Road, Kolkata 700 032, India

Received 24 August 2009; received in revised form 24 September 2009; accepted 26 November 2009

Available online 4 January 2010

Abstract

MgO–Al₂O₃–TiO₂ based glass–ceramic coatings were formed on nimonic superalloy substrates by microwave and conventional heat treatment processes. The resultant glass–ceramic coatings were characterized by X-ray diffractometry (XRD), scanning electron microscopy (SEM), image analysis, nanohardness and Young's modulus evaluation by depth sensitive indentation (DSI) technique. Nanohardness and Young's modulus values of the microwave heat treated glass–ceramic coatings were improved in comparison to those of the conventionally treated glass–ceramic coatings due to presence of finer sized crystallites in the microwave processed coatings. Slight enhancement in the nanohardness and Young's modulus values with soaking time for the microwave processed coatings were explained in terms of the microstructural refinement and the reinforcement of the parent glass matrix.

© 2009 Elsevier Ltd and Techna Group S.r.l. All rights reserved.

Keywords: A. Microwave processing; B. Electron microscopy; C. Mechanical properties; D. Glass ceramics

1. Introduction

The application of microwave energy is emerging as an innovative technology for the processing of materials in an efficient, economic and effective manner [1–5]. Microwave heating has been utilized for the novel processing of materials, e.g. glazing of coating, joining of ceramic materials, preparation of nanomaterials, development of functionally graded materials (FGMs), synthesis of ceramic powder, sintering of metal powder and crystallization of glass, etc. [6–13].

We have reported on the development of oxide coating on Al and Al–Al₂O₃ composite using microwave heating [14–16]. High temperature and abrasion resistant glass–ceramic coatings have been developed from a glass in the MgO–Al₂O₃–TiO₂ system for nickel based superalloy substrates for applications in different hot zone components of gas turbine engine and reported elsewhere [17]. The objective of the present work was to obtain glass–ceramic coating on a nickel based superalloy substrate by microwave processing and evaluate the coating.

2. Experimental

A glass composition was selected from the MgO–Al₂O₃–TiO₂ system (composition shown in Table 1). To prepare the glassy material, the glass-forming batch was melted at 1400 °C for 2 h and subsequently the molten glass was fritted. The frit was ground to powder, which was subjected to differential thermal analysis (STA 409 C/CD, Netzsch, Germany) to determine the nucleation and the growth temperatures of the crystallites. The glass powder was wet milled with the mill addition of 5 wt.% clay in a porcelain ball mill for 45 h to obtain fine glass particles (average size 3–5 μm). Suitable glass slurry was produced for application on the cleaned metal surface. The glass slurry was applied on the nickel based superalloy substrates, Nimonic – AE 435 (composition shown in Table 2) using conventional spraying technique, which were subsequently dried at 100 °C for 1 h and thereafter fired at 1165 °C for 6 min in a muffle furnace [17]. The thickness of the glass coating was ~100 μm.

The glass coated nimonic alloy substrates were heat treated in a microwave furnace (Multilab 2.0 kW, 2.45 GHz, Linn High Therm GmbH, Germany) at 863 °C (nucleation temperature) for 30–90 min followed by 30–90 min at 958 °C (growth temperature). The samples were placed in a silicon carbide

^{*} Corresponding author. Tel.: +91 033 2473 3469/76/77/96;
fax: +91 033 2473 0957.

E-mail addresses: sumana@cgcricri.res.in, jttian@ouc.edu.cn (S. Das).

Table 1
Glass composition.

Oxides	Wt. %
SiO ₂	32
Na ₂ O	2
K ₂ O	5
TiO ₂	13
B ₂ O ₃	10
MgO	12
CaO	2
Al ₂ O ₃	24

crucible, which acted as susceptor. The whole assembly was thermally insulated by alumina fibre boards. Initially, silicon carbide absorbed the microwave energy and increased the temperature of the glass coating. Beyond a critical temperature ~ 800 °C, the relative dielectric constant and the loss tangent values of the glass coating increased remarkably that facilitated effective coupling of the glass coating with the microwave energy resulting in processing of the coating [1]. The temperature was measured using an optical pyrometer having an accuracy of $\pm 1\%$. Conventional heat treatments of the glass coated nimonic alloy substrates were carried out in a muffle furnace following identical heat treatment schedules as were adopted for microwave heat treatments for comparison.

The phase composition of the microwave and conventional processed glass–ceramic coatings was determined by X-ray diffractometry (PW 1710, Philips Research Laboratory, Eindhoven, The Netherlands) using Cu K α radiation (45 kV, 35 mA). The surface microstructure of the same coatings was examined by scanning electron microscopy (SEM, LEO S430i, LEO, UK). Crystallite size and area fraction of the crystalline phases of the identical glass–ceramic coatings were estimated by image analysis technique (LEICA Q500MC, UK) using five SEM micrographs for each sample type. Nanohardness and Young's modulus of the corresponding coatings were measured for five samples of each given type by depth sensitive indentation (DSI) technique (Fischerscope H100C XY_p, Fischer, Switzerland).

Nanohardness and Young's modulus of the microwave and conventionally processed glass–ceramic coatings were determined from the load–displacement plots following the already established methods [18,19]. Nanoindentation was done on the

Table 2
Nominal composition of the Nimonic superalloy (AE 435) in wt. %.

Elements	Wt. %
Cr	19–22
Fe	1.0
C	0.12
Si	0.8
Mn	0.7
Ti	0.15–0.35
Al	0.15
Cu	0.07
S	0.01
P	0.015
Ni	Balance

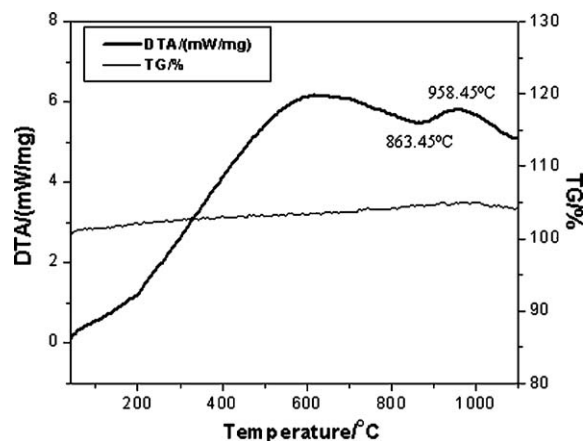


Fig. 1. DTA and TG curves of glass.

flat parallel, polished coating surface using the depth sensitive indentation machine as mentioned above. A four-sided diamond pyramidal Vicker's tip with a nominal radius of curvature around 130 nm was used as the indenter. The load and the displacement were monitored by a three-plate capacitive force/displacement transducer continuously. The force sensing and depth sensing resolution were 0.2 μ N and 0.1 nm, respectively. Indentations were conducted at 1 mN and

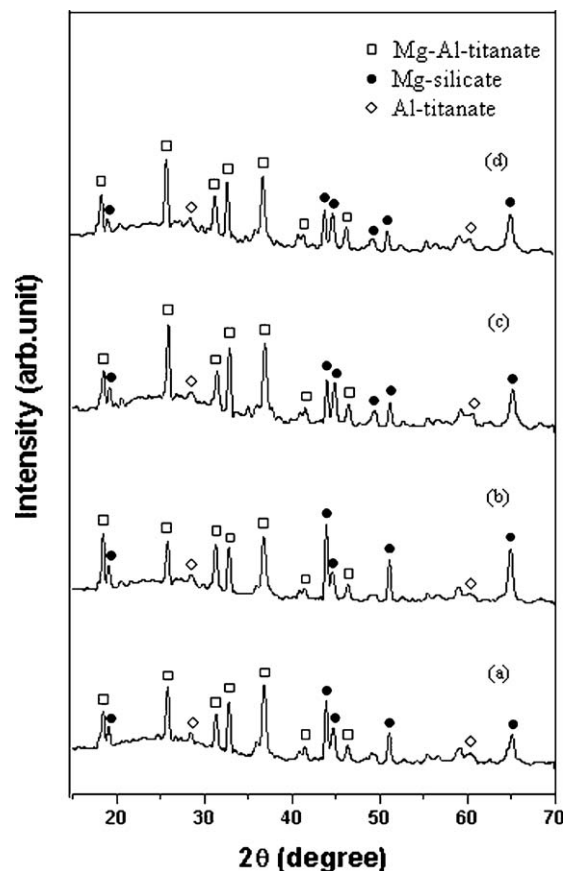


Fig. 2. XRD patterns of glass–ceramic coatings heat treated for (a) 30 min at 863 °C followed by 30 min at 958 °C, microwave; (b) 30 min at 863 °C followed by 30 min at 958 °C, conventional; (c) 90 min at 863 °C followed by 90 min at 958 °C, microwave; and (d) 90 min at 863 °C followed by 90 min at 958 °C, conventional.

1000 mN loads with the loading and unloading times of 30 s each. The load was selected according to the thumb rule that the maximum depth of penetration of the indenter into the coating must be well below 10% of the coating thickness in order to avoid the effect of the mechanical properties of the substrate into the data measured for the coating. To ensure statistical validity a large number of data were taken for each sample type.

3. Results and discussion

3.1. DTA and TGA

Fig. 1 shows the DTA and TG curves of the glass. The DTA data show that the nucleation and the growth temperatures are 863.45 °C and 958.45 °C, respectively. From the TG curve it can be seen that negligible mass gain occurred up to 1100 °C.

3.2. XRD and SEM observations

Magnesium aluminium titanate ($\text{MgAl}_2\text{Ti}_3\text{O}_{10}$), magnesium silicate (MgSiO_3) and aluminium titanate (Al_2TiO_5) crystalline phases were identified in all the glass–ceramic coatings obtained by the microwave and conventional heat treatments. Typical XRD patterns of the microwave and conventionally processed glass–ceramic coatings are shown in Fig. 2a–d. It was observed from the SEM surface microstructures that the

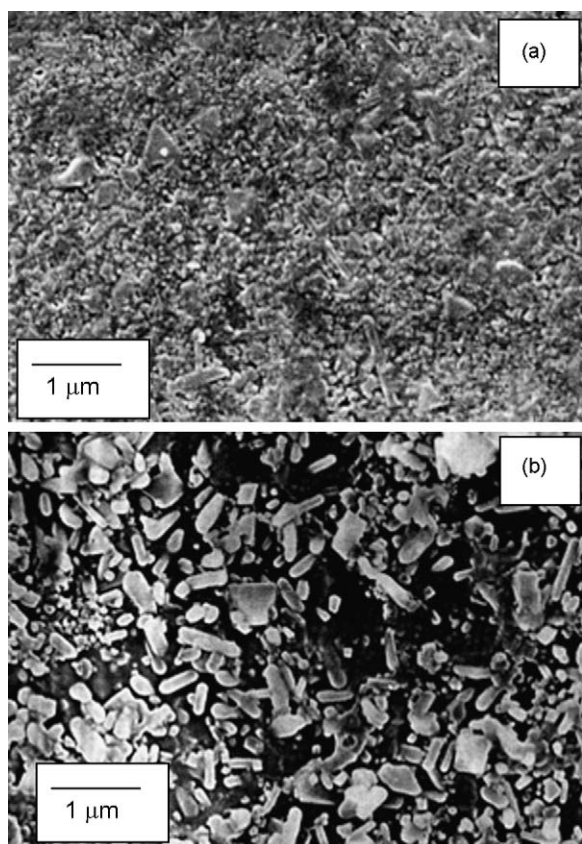


Fig. 3. Microstructures of microwave and conventionally processed glass–ceramic coatings for 90 min at 863 °C followed by 90 min at 958 °C: (a) microwave and (b) conventional.

microwave processing produced finer sized crystallites in the coatings compared to the sizes of the crystallites obtained in the conventionally processed coatings under all processing conditions. For 90 min soaking time at the processing temperatures, the average crystallite size (~ 195 nm) was quite lower in the microwave processed coating than that (~ 410 nm) for the conventionally processed coating (Fig. 3a and b).

3.3. Nanohardness measurements

Fig. 4a and b shows the typical load–deflection curves of the glass–ceramic coatings microwave and conventionally processed for 90 min at 863 °C followed by 90 min at 958 °C at the test load of 1000 mN. The data on nanohardness for the glass–ceramic coatings obtained by microwave and conventional processing techniques using different heat treatment conditions at a test load of 1 mN are shown in Fig. 5a. The data show that the nanohardness values (5.68–6.12 GPa) of microwave processed coatings measured at a test load of 1 mN were higher than those (4.25–5.23 GPa) of the coatings obtained by

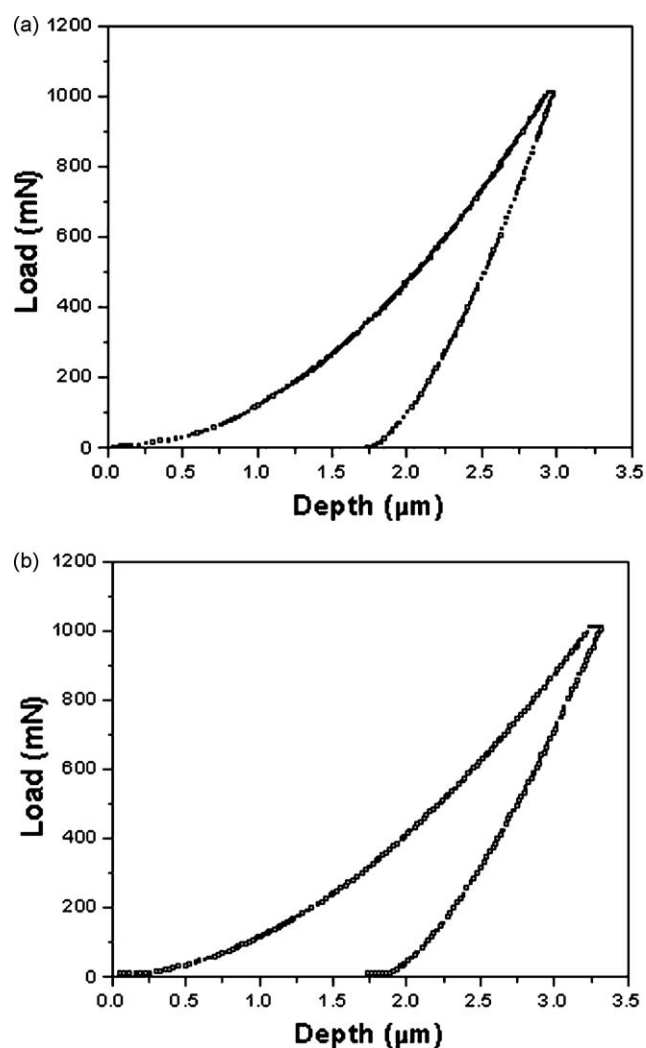


Fig. 4. Typical load–deflection curves of microwave and conventionally processed glass–ceramic coatings for 90 min at 863 °C followed by 90 min at 958 °C: (a) microwave and (b) conventional (test load: 1000 mN).

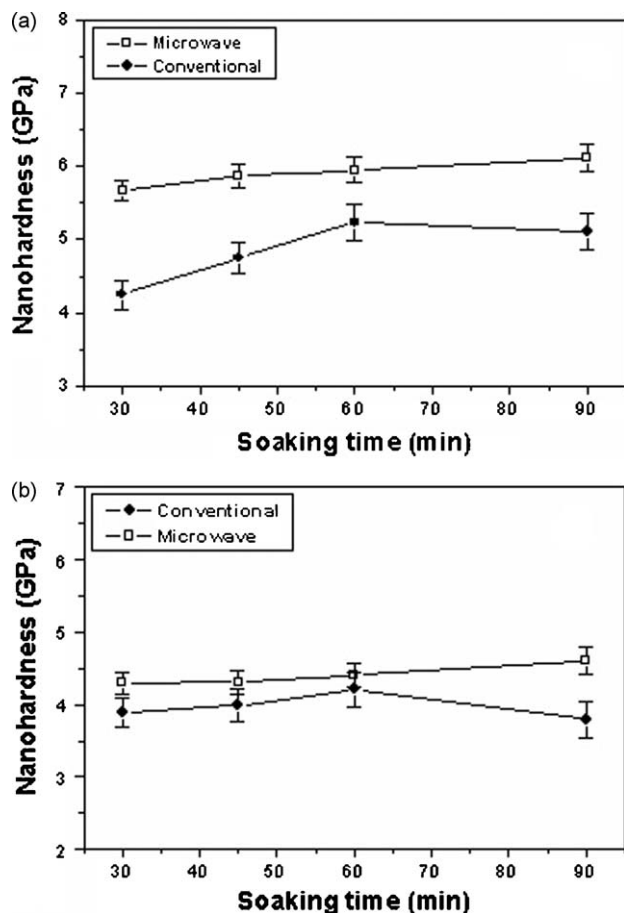


Fig. 5. Nanohardness of microwave and conventionally processed glass–ceramic coatings: (a) test load: 1 mN and (b) test load: 1000 mN.

the conventional heat treatments for all the soak times (30–90 min). The nanohardness values of the microwave treated coatings slightly enhanced with increasing the soaking time. Further, it can be noted that in the case of conventionally processed coatings, the nanohardness values initially increased and then decreased with increasing soaking time beyond 60 min (e.g. 90 min). Fig. 5b shows the nanohardness values at a test load of 1000 mN for microwave and conventionally processed glass–ceramic coatings as a function of soaking time. The trend was similar as that observed in Fig. 5a. The nanohardness values of the microwave processed glass–ceramic coatings were in the range of 4.29–4.61 GPa for 30–90 min soaking time. On the other hand, the nanohardness values were 3.89–4.21 GPa for the conventionally processed coatings for all the soak times (30–90 min). Fig. 6a and b shows the nanoindentation arrays at 1000 mN applied load in the glass–ceramic coatings microwave and conventionally heat treated for 90 min at 863 °C followed by 90 min at 958 °C. Fig. 6 also indicates that the microwave processed coating had smooth surface compared to that of the conventionally processed coating under identical processing conditions.

The nanohardness values of the microwave treated glass–ceramic coatings were higher than those of the conventionally processed ones, most probably because of their finer crystallite

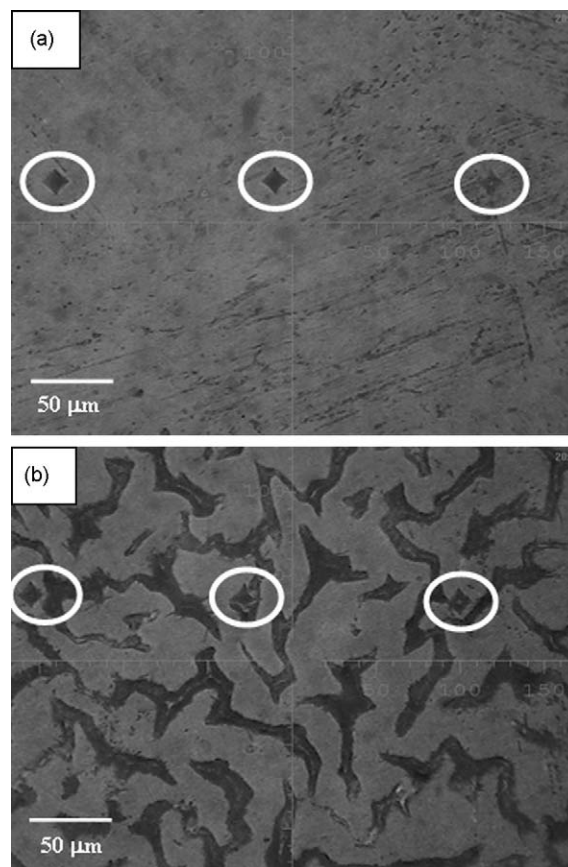


Fig. 6. Nanoindentation arrays at 1000 mN applied load in microwave and conventionally processed glass–ceramic coatings for 90 min at 863 °C followed by 90 min at 958 °C: (a) microwave and (b) conventional (magnification: 20×).

sizes. The slight increase in the nanohardness values with the soaking time for the microwave processed coatings was most likely linked to the decrease in crystallite size and the consequent increase in their area fraction with the increase in soaking time (Fig. 7a) [13,20,21]. As the area fraction of the crystallites increased with the soaking time, the extent of reinforcement to the glass matrix increased, which resulted in the enhancement of nanohardness in the microwave processed coating. In the conventionally processed coatings, the nanohardness values decreased at higher soaking time (e.g. 90 min) due to larger crystallite size (Figs. 7b and 3b) leading to decrease in their area fraction (Fig. 7b) and thereby, the extent of reinforcement to the glass matrix decreased.

3.4. Young's modulus measurements

The Young's modulus values (92.62–96.88 GPa) of the microwave processed glass–ceramic coatings were higher than those (72.56–84.5 GPa) of the conventionally processed glass–ceramic coatings at 1 mN applied load (Fig. 8a). The Young's modulus values of the microwave processed coatings slightly increased with the soak time. It can be further observed that in the conventionally processed coatings the Young's modulus values initially increased and then decreased with increasing

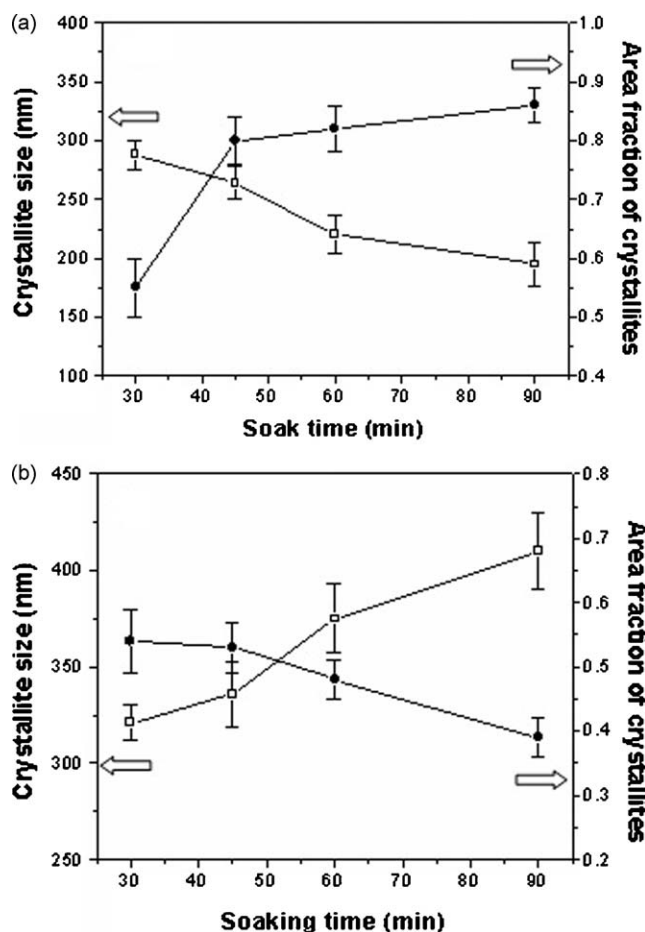


Fig. 7. Crystallite size and area fraction of crystalline phases versus soaking time curves for microwave and conventionally processed glass–ceramic coatings: (a) microwave and (b) conventional.

soaking time beyond 60 min (e.g. 90 min). Fig. 8b shows the Young's modulus values at a test load of 1000 mN for microwave and conventionally processed glass–ceramic coatings. The trend of data was similar as that observed in Fig. 8a. The Young's modulus values of the microwave processed coatings were in the range of 92.21–96.75 GPa for 30–90 min soaking time (Fig. 8b). On the other hand, the Young's modulus values were 72.45–84.43 GPa for the coatings obtained by the conventional heat treatments for all the soak times (30–90 min) (Fig. 8b).

The increase in Young's modulus with the soak time in the case of microwave processed coating is expected as the area fraction enhancement of fine crystallites with the soaking time (Fig. 7a) provided more rigidity and localized strong bonding. The average crystallite sizes of the conventionally treated coatings actually increased with the soaking time and as a result, the area fractions of the crystallites decreased (Fig. 7b). This explains why the conventionally processed coatings showed lower Young's modulus values than those of the microwave heat treated coatings [22,23]. The Young's modulus values of the conventionally treated coatings decreased at higher soaking time (e.g. 90 min) due to decrease in the area fraction of the crystalline phases on account of larger crystallite size (Figs. 7b and 3b).

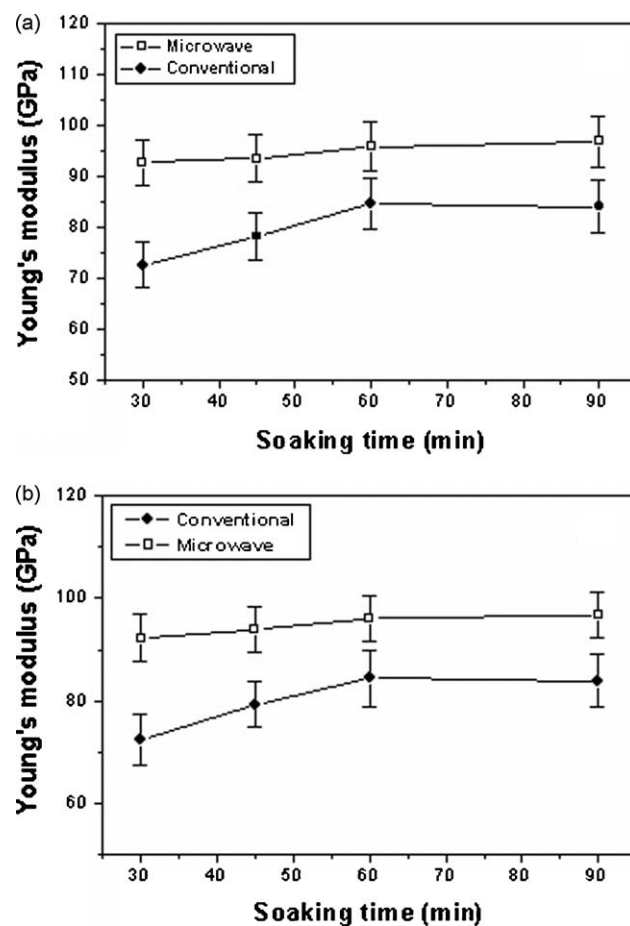


Fig. 8. Young's modulus of microwave and conventionally processed glass–ceramic coatings: (a) test load: 1 mN and (b) test load: 1000 mN.

4. Conclusions

Considerable improvement in the nanohardness as well as Young's modulus was observed in the case of microwave processed glass–ceramic coatings compared to that of the conventionally heat treated coatings. The experimental results further indicate that microwave processing can be efficiently utilized to tailor the microstructure and properties of the glass–ceramic coating for a chosen application.

Acknowledgements

The authors are very grateful to Dr. H.S. Maiti, Director, Central Glass and Ceramic Research Institute (C.G.C.R.I.), Kolkata 700 032, India, for his kind permission to publish this paper. The authors are also thankful to Dr. S. Majumder, Mr. A.K. Mandal, Mr. S.K. Dalui, Mr. A. Karmakar and Mr. B. Chakraborty for XRD, SEM, image analysis and other experiments.

References

- [1] W.H. Sutton, Microwave processing of ceramic materials, *Ceram. Bull.* 68 (1989) 376–386.

- [2] A.K. Mukhopadhyay, M. Ray Chaudhury, A. Seal, S.K. Dalui, M. Banerjee, K.K. Phani, Mechanical characterization of microwave sintered zinc oxide, *Bull. Mater. Sci.* 24 (2001) 125–128.
- [3] S. Mandal, A. Seal, S.K. Dalui, A.K. Dey, S. Ghatak, A.K. Mukhopadhyay, Mechanical characteristics of microwave sintered silicon carbide, *Bull. Mater. Sci.* 24 (2001) 121–124.
- [4] A.R. Boccaccini, P. Veronesi, C. Leonelli, Microwave processing of glass matrix composites containing controlled isolated porosity, *J. Eur. Ceram. Soc.* 21 (2001) 1073–1080.
- [5] S. Aravindan, R. Krishnamurthy, Joining of ceramic composites by microwave heating, *Mater. Lett.* 38 (1999) 245–249.
- [6] A.K. Sharma, S. Aravindhan, R. Krishnamurthy, Microwave glazing of alumina–titania ceramic composite coatings, *Mater. Lett.* 50 (2001) 295–301.
- [7] L. Zeng, E.D. Case, M.A. Crimp, Effects of a silica spin-on interlayer and heating mode on the joining of zirconia and MaCorTM, *Mater. Sci. Eng. A* 357 (2003) 67–74.
- [8] S.K. Apte, S.D. Naik, R.S. Sonawane, B.B. Kale, N. Pavaskar, A.B. Mandale, B.K. Das, Nanosize Mn_3O_4 (hausmannite) by microwave irradiation method, *Mater. Res. Bull.* 41 (2006) 647–654.
- [9] M. Cirakoglu, S. Bhaduri, S.B. Bhaduri, Processing and characterization of Ti–B-based functionally graded materials produced by microwave-activated combustion synthesis, *J. Mater. Res.* 17 (2002) 2823–2830.
- [10] Y.-P. Fu, Microwave-induced combustion synthesis of $\text{Li}_{0.5}\text{Fe}_{2.5-x}\text{Cr}_x\text{O}_4$ powder and their characterization, *Mater. Res. Bull.* 41 (2006) 809–816.
- [11] W.L.E. Wong, M. Gupta, Development of Mg/Cu nanocomposites using microwave assisted rapid sintering, *Compos. Sci. Technol.* 67 (2007) 1541–1552.
- [12] A.D. Cozzi, Z. Fathi, D.E. Clark, Crystallization of sol–gel derived barium aluminosilicate in a 2.45 GHz microwave field, in: D.E. Clark, W.R. Tinga, J.R. Laia, Jr. (Eds.), *Microwaves: Theory and Application in Materials Processing II*, Ceramic Transactions, vol. 36, The Am. Ceram. Soc., Inc., Westerville, OH, 1993, pp. 317–324.
- [13] C. Siligardi, C. Leonelli, F. Bondioli, A. Corradi, G.C. Pellacani, Densification of glass powders belonging to the $\text{CaO–ZrO}_2\text{–SiO}_2$ system by microwave heating, *J. Eur. Ceram. Soc.* 20 (2000) 177–183.
- [14] S. Das, A.K. Mukhopadhyay, S. Datta, D. Basu, Novel method of developing oxide coating on aluminium using microwave heating, *J. Mater. Sci. Lett.* 22 (2003) 1635–1637.
- [15] S. Das, A.K. Mukhopadhyay, S. Datta, D. Basu, Aluminium oxide coating by microwave processing, *Trans. Ind. Ceram. Soc.* 65 (2006) 105–110.
- [16] S. Das, D. Basu, S. Datta, A.K. Mukhopadhyay, A process of making Al– Al_2O_3 composites useful in engineering applications, Indian Patent application, Appl. No. 245/DEL/03.
- [17] S. Datta, S. Das, A new high temperature resistant glass–ceramic coating for gas turbine engine components, *Bull. Mater. Sci.* 28 (2005) 689–696.
- [18] N.K. Mukhopadhyay, P. Paufler, Micro and nanoindentation techniques for mechanical characterisation of materials, *Int. Mater. Rev.* 51 (2006) 209–245(37).
- [19] W.C. Oliver, G.M. Pharr, An improved technique for determining hardness and elastic modulus using load and displacement sensing indentation experiments, *J. Mater. Res.* 7 (1992) 1564–1583.
- [20] R.M. Fulrath, Internal stress in model ceramic systems, *J. Am. Ceram. Soc.* 42 (1959) 423–429.
- [21] C. Xu, Effects of particle size and matrix grain size and volume fraction of particles on the toughening of ceramic composite by thermal residual stress, *Ceram. Int.* 31 (2005) 537–542.
- [22] R.J. Cardoso, A. Shukla, A. Bose, Effect of particle size and surface treatment on constitutive properties of polyester–cenosphere composites, *J. Mater. Sci.* 37 (2002) 603–613.
- [23] S.N. Nazhat, R. Joseph, M. Wang, R. Smith, K.E. Tanner, W. Bonfield, Dynamic mechanical characterization of hydroxyapatite reinforced polyethylene: effect of particle size, *J. Mater. Sci.: Mater. Med.* 11 (2000) 621–628.